Study of the integration of a supersonic impulse turbine in a NH_3/H_2O absorption heat pump for combined cooling and power production from a low temperature heat source.

Simone Braccio[1,2,*], *Hai Trieu* Phan[1], *Nicolas* Tauveron[1], and *Nolwenn* Le Pierrès[2]

[1]Univ. Grenoble Alpes, CEA, LITEN, DTCH. F-38000 Grenoble, France
[2]Laboraty LOCIE, Université Savoie Mont Blanc CNRS UMR 5271, 73376 Le Bourget Du Lac, France

Abstract. The present work is focused on the investigation of an absorption cycle integrated with an impulse axial turbine for the combined production of cooling and electric power. This technology holds great promise for its ability to harness low-temperature heat sources, more efficiently in comparison to separate production with simple cycles. By developing a 1D model of the expander, and integrating it into a 0D model of the complete cycle, it is possible to evaluate the performance of the cycle and its variation with respect to the operating parameters, namely the temperature of the external resources. Pending an experimental validation of the results, this study showed the importance of correctly defining the temperature of the sources - namely the generator temperature - in order to satisfy the technological needs while also maximising the efficiency of the cycle. Finally it was highlighted how the integration of a supersonic impulse turbine strongly limits the flexibility during operation given the constant mass flow rate treated by the expander.

1 Introduction

In view of the ever increasing global demand for energy, research is increasingly being developed on new, more efficient energy conversion technologies based on renewable or recovered sources. In this context, absorption systems [1] are well suited for the recovery of energy at low temperature for the production of cooling. Combined cycles using the same working fluid for the co-production of cold and electricity are even more interesting for improving energy efficiency.

Different architectures of combined cold and electricity production systems are described in literature [2]. Two families can be distinguished: series architectures [3]-[4] and parallel architectures [5]-[6]-[7]. The former are generally more efficient while the latter offer more flexibility between the different production methods and are easier to implement. Regardless of the architectures, cold can be produced using the principle of absorption machines [6]-[8]-[9] or that of ejectors [3] or even a combination of the two technologies [9]-[10]. Electricity is produced by the expansion of the working fluid in a volumetric type expander or turbine [11].

The present work focuses on a low temperature parallel combined cooling and power (CCP) production system based on a water/ammonia absorption machine. The study is based

*corrresponding author: simone.braccio@cea.fr

on an experimental pilot plant [12] present at CEA Ines since 2011 (Figure 1) that works very well for the cooling production and to which an expander is being integrated. The power of the generator is 15 kW and a target electric power 1 kW. In a previous study [13], the expander initially selected (a scroll type volumetric expander) was found to be unsuitable for such a small size application due to an excessive leakage rate. A different power generation technology is therefore investigated here, that of a partial admission action turbo-expander. The fact that in this type of expander all the expansion takes place in the distributor should limit the influence of leaking losses and guarantee a good level of work output [14]. However, due to the intrinsic behavior of the machine, special attention must be paid to the interdependence between the physics governing the expander and the cycle in which it is integrated.

Figure 1. Picture of the pilot plant.

2 Cycle description

The combined cycle considered in this study is shown in Figure 2. The functioning is that of a water-ammonia absorption machine to which a turbine is coupled in parallel with the cooling production. On the solution side, a first line of solution rich in ammonia circulates from the absorber to the generator and is pressurized by a pump. A second line comprising an expansion valve returns the poor solution to the absorber. An economizer allows preheating the rich solution thanks to the poor solution heat. In the generator, a supply of heat at low temperature allows the desorption of steam, mainly consisting of ammonia, from the solution. The division of the steam flows is done directly at the exit of the generator so that the rectification (purification of the steam from the water it contains) only takes place on the cold line in order to maximize both cooling and power production. This configuration was chosen following previous studies on the optimal position of the rectifier [12].

On the electricity production side, the expander selection process leads to the identification of a partial admission impulse turbine as the best choice for the application, given the specific speed and specific diameter calculated to be respectively around 5 and 13 [15]. The turbine considered in this study for the production of the power $\dot{W}_t$ is therefore an axial micro turbine characterized by a distributor composed of a single converging-diverging injector. Before the turbine, a superheater provides the power $\dot{Q}_{sh}$, to increase the temperature of the

fluid to ensure that it remains in the gas state throughout the expansion in the turbine. In fact, the condensation of the mixture during the expansion would be a detrimental factor for good functioning of the expander and could lead to its breaking.

On the cold production side, ammonia is condensed by exchanging the thermal power $\dot{Q}_c$ with an intermediate temperature source (generally ambient air). Before cooling the cold source at the evaporator by absorbing the power $\dot{Q}_e$, the fluid is expanded in a valve to reach low pressure. A sub-cooler is used to pre-cool the ammonia before it expands by using the ammonia coming out from the evaporator.

The flows from the two production lines get mixed and are finally absorbed in the poor solution thanks to cooling by an intermediate source to which the power $\dot{Q}_a$ is transferred.

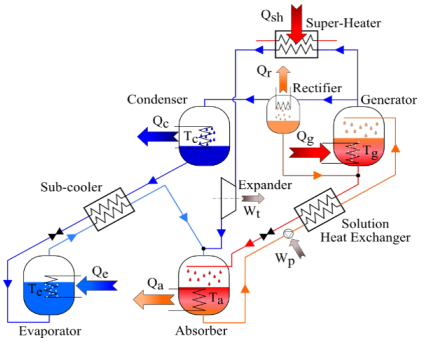

Figure 2. Scheme of the combined cycle

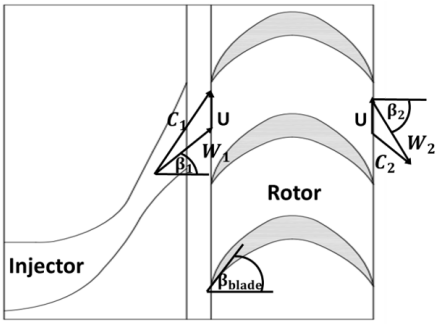

Figure 3. Scheme of the turbine

3 Expander Model

The expander considered in the present study (Figure 3) is a partial admission supersonic axial turbine with a single convergent-divergent injector, which converts the entire enthalpy drop into kinetic energy, resulting in a zero reaction degree. Taking into account the very low steam mass flow rates available, the choice of a partial admission machine helps avoiding too small dimensions or excessive rotation speeds. In addition, the fact that all the expansion takes place in the distributor and that there is no pressure drop in the rotor, avoids the loss of performance due to leaking losses which can become very penalizing for machines of this size.

A compressible 1D model of the turbo-expander was created in EES - Engineering Equation Solver - [16]. The behavior as a real gas and a two-phase mixture of the fluid is taken into account thanks to correlations describing the thermodynamic state of the water-ammonia mixture [17]. In the calculation of the sonic conditions and of the treated mass flow rate, the condensation of the mixture during the expansion is taken into account by making the enthalpy balance under the assumption that the liquid phase and the vapor phase are at the same temperature $T_{liq,sat} = T_{vap,sat}$ and that the condensing mixture is entrained by the vapor, so that the two have the same velocity ($C_{liq,sat} = C_{vap,sat} = C_{mixture}$). In addition, only the speed of sound of the saturated vapor was taken into account for purpose of calculation of the critical conditions of the mixture.

Depending on the operating conditions, a variable percentage of water remains in the steam produced by the generator. The influence of the ammonia mass fraction in the mixture entering the turbine on the flow rate passing through it was first analyzed. The range of ammonia concentrations in the refrigerant vapor that can be found in the cycle (rarely less

than 90%) has little influence on the mass flow rate treated by the distributor: for example for inlet conditions of 12 bar and 120 °C there is a maximum reduction of 3.15% in the case of a mixture with an ammonia mass fraction of 90% compared to the case of pure ammonia.

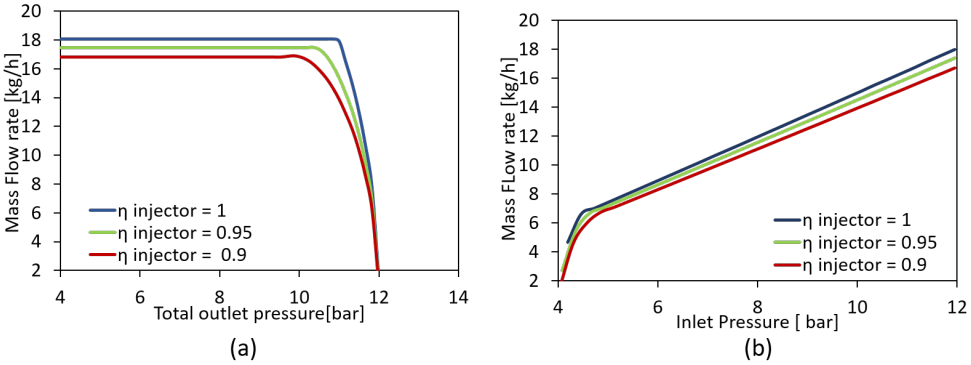

Figure 4. Turbine mass flow rate characteristic fixing the total inlet pressure equal to 12 bar (a), and total outlet pressure equal to 4 bar (b)

Figures 4a and 4b show the injector mass flow rate characteristic as a function of the total outlet pressure, setting the total inlet pressure (Figure 4a) and vice versa (Figure 4b) for different isentropic efficiencies of the injector in the case of pure ammonia.

A slight pressure difference is sufficient to achieve the blocking condition and maximum flow through the sonic section of the injector. In the case of injector isentropic efficiency equal to one, the outlet to inlet pressure ratio sufficient to achieve sonic conditions in the minimum section, β_{lim}, is equal to 0.916, close to that calculable by the classical relations of ideal gases using an adiabatic index $k = c_p/c_v$ defined as the arithmetic mean of the values relating to upstream and downstream conditions [18]. As the isentropic efficiency of the injector decreases, the β_{lim} required to achieve sonic conditions decreases as does the maximum flow rate treated. In fact, lower injector efficiciencies correspond to greater total pressure losses and therefore to a greater pressure variation necessary to reach the critical conditions. On the other hand, these conditions correspond to lower pressures and higher temperatures resulting in a decrease in fluid density and mass flow. The isentropic efficiency of the injector also has a strong influence on the entry velocity into the rotor and is therefore a determining factor for the overall efficiency of the machine. Figure 4b shows the same flow characteristic, setting the pressure downstream of the injector and varying that upstream.

An energy balance allows calculating the entry speed into the rotor; this is used to find the ideal work W_{id} exchanged by the fluid with the moving blades using Euler equation [19] $W_{id} = U(C_{u1} - C_{u2})$. The velocities triangle is shown in 3, where U indicates the rotation speed of the turbine, C_1, W_1 and β_1 are the absolute velocity,relative velocity and angle of the relative velocity at the rotor inlet, C_2, W_2 and β_2 are the same quantities at the exit of the rotor, and β_{blade} is the constructive angle of the blade. From the maximum theoretical work that can be produced from the input kinetic energy, loss terms must be subtracted. These are commonly divided into incidence loss, passage loss, friction loss and windage loss. The partialization increases the loss term due to the ventilation effect and if the turbine is strongly partialized, the blades only stay in the active region for a short time, making full intake losses negligible compared to the partial intake ones [20].

The incidence losses are expressed as follows [21]:

$$\Delta h_i = \frac{1}{2}\cos^2(\beta_1 - \beta_{blade})W_1^2 \tag{1}$$

Passage losses due to friction in the blade channels are taken into account as [22]:

$$\Delta h_p = \frac{1}{2}(1 - \Psi^2)W_1^2 \tag{2}$$

where $\Psi = 0.99 - \frac{2.28\Delta\beta}{10^4} - \frac{4.97}{180-\Delta\beta}$ and $\Delta\beta = \beta_1 - \beta_2$

The windage loss is calculated as follows [23]:

$$\Delta h_w = \frac{k_w d_m b_1 \epsilon \rho U^3}{\dot{m}} \tag{3}$$

where ρ is the density in the rotor, b_1 is the height of the blade, d_m the average diameter of the rotor, U is rotational speed of the turbine and $k_w = 0.6\sqrt{b_1}$.

Finally, introducing a coefficient $k_d = 1.2 \cdot 10^{-3}$ loss due to the friction on the disc is [23]:

$$\Delta h_d = \frac{k_d d_m^2 \rho U^3}{\dot{m}} \tag{4}$$

The total to total isentropic efficiency of the turbine is therefore calculated as follows:

$$\eta_{tt} = \frac{W_{id} - \Delta h_i - \Delta h_p - \Delta h_w - \Delta h_d}{\Delta h_{is}} \tag{5}$$

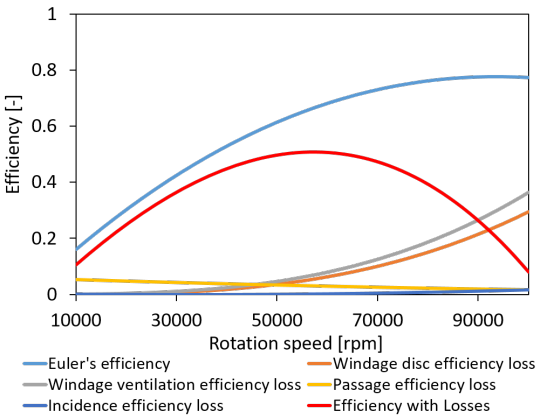

Figure 5. Turbine efficiency characteristic with pure ammonia for inlet condition of 120 °C and 12 bar and outlet pressure of 5 bar

The results of the model for pure ammonia are presented in Figure 5. Due to the small size of the turbine and the strong partial admission rate (i.e. the ratio of the number of active blades to the total) $\epsilon = 3.7\%$, the partial intake losses become preponderant with respect to all the others above a certain rotation speed. It can also be seen that for high rotation speeds, the windage losses associated with the partialization take an increasingly large value, shifting

the maximum efficiency of the turbomachine (52%) to lower rotation speeds compared to the theoretical curve, obtained in the absence of losses in the rotor, from about 100,000 rpm to about 60,000 rpm.

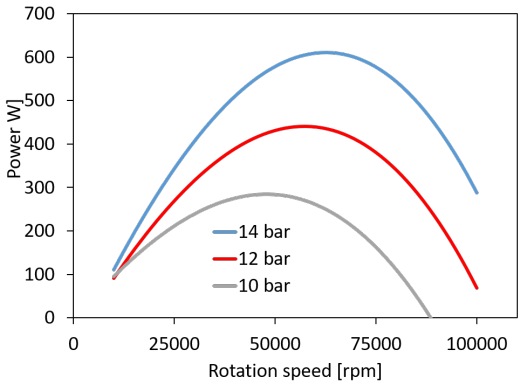

Figure 6. Turbine power characteristic with pure ammonia for an inlet temperature of 120 °C and outlet pressure of 5 bar for different inlet pressure values

Figure 6 shows the power produced by the turbine for different inlet pressure values. As the inlet pressure increases, the power produced also increases, and its maximum value moves to higher rotation speeds.

4 Integrated cycle model

A numerical model of the presented absorption cycle was developed. For each component, the energy and mass balance equations are formulated under the steady state assumption. The model of heat exchangers is based on fixed pinch point values, pressure drops and efficiency determined from previous experimental experiences [23] and it is assumed that the mixture is at saturation at the outlet of each exchanger (except for an imposed superheating at the evaporator outlet). To complete the development of the combined cycle, the turbine model is integrated into the absorption machine model, together with a superheater, modeled as an adjustable power supply to the fluid. To estimate the efficiency of the cold production of the cycle, the cooling COP is defined as follows:

$$COP = \frac{\dot{Q}_e}{\dot{Q}_g \cdot r_s} \tag{6}$$

where in the denominator the power supplied at the generator $\dot{Q}_g$ is multiplied for the ratio r_s between the mass flow rate passing through the evaporator and the vapour mass flow rate desorbed at the generator, to take into account the fact that not all the vapour produced is used for the production of the cooling power $\dot{Q}_e$. On the other hand, the efficiency of the power cycle is calculated as follows:

$$\eta_{power} = \frac{\dot{W}_t}{\dot{Q}_g \cdot (1 - r_s) + \dot{Q}_{sh}} \tag{7}$$

Table 1 shows the strong impact that the integration of the turbine has on the cycle even at the nominal operating point, characterized by a generator temperature T_g = 100°C and power $\dot{Q}_g$ = 15 kW, ambient temperature T_a = 25°C and cooling production temperature T_e = 5°C. In fact, once the turbine line is open, much of the mass flow rate produced by the generator is deviated towards the expander, whose treated mass flow rate solely depends on the inlet- outlet pressure difference. The refrigerant vapour mass flow rate division between the turbine and evaporator lines has a strong impact on the power exchanged by the various heat exchangers but has no influence on the high and low pressure of the cycle, defined respectively by the condenser and evaporator temperature. Also the ammonia concentration in the different parts of the cycle remains unaffected by the presence of the turbine, with the only difference that, as the rectification takes place after stream division, the ammonia concentration on the power line remains the same as the one at the generator outlet.

	$\dot{Q}_a$ [kW]	$\dot{Q}_c$ [kW]	$\dot{Q}_e$ [kw]	$\dot{W}_t$ [kW]	$\dot{Q}_{sh}$ [kW]	$\dot{m}_{evap}$ [kg/h]	$\dot{m}_{turb}$ [kg/h]
Turbine line closed	12.38	9.83	9.21	0	0	28.2	0
Turbine line open	13.62	4.39	4.06	0.45	0.30	12.45	17.13

Table 1. Influence of the turbine on the cycle at the nominal operating point.

First, the influence of the generator on the cycle is studied in terms of power supplied and temperature. If a generator temperature is set, there is a minimum power to supply it to be able to produce the steam mass flow rate required by the turbine. When the power supplied to the generator increases, the mass flow rate of produced steam increases and, as the mass flow rate treated by the turbine in chocking conditions does not change, the value of the ratio r_s must increases as well as the mass flow passing through the refrigeration cycle and therefore the cooling power produced.

For a set power supplied to the generator, a higher generator temperature implies a reduction in the mass flow rate of steam produced because of the higher sensible heat transferred to the solution, resulting in a decrease in the mass flow circulating in the cold part of the circuit. Therefore, the minimum generator power for the cycle to operate in combined mode increases from 8.5 kW for generator temperatures of 100 °C to about 10 kW for temperatures of 150 °C. The above was obtained under the assumption of a cooling demand at 0 °C. Equation 6 shows that the cooling power produced is proportional to the percentage mass flow rate passing through the cold part of the circuit (r_s), but also to the COP, whose increasing - decreasing tendency with the generator temperature T_g depends strongly on the cooling production temperature T_e.

The cooling production temperature is indeed a fundamental parameter in the characterization of the behavior of the cycle and exerts a strong influence on the electrical and cooling power produced by the cycle, on its efficiency and on the optimum temperature of the hot source as shown in Figure 7a and Figure 7b, where the power supplied at the generator is of 10 kW and the ambient temperature 25°C.

The influence of the condensation temperature T_c on the cycle (Figure 8) is then analyzed. An increase in this intermediate temperature leads to an increase in the maximum cycle pressure and thus in the pressure ratio available to the turbine. Therefore the power produced and the mass flow rate treated by the expander increase significantly. On the contrary, the cooling power produced undergoes a decrease due to the lower mass flow rate circulating through the cold part of the cycle, and the change in the COP. On the other hand, an increase in the tem-

perature of the evaporator, has a positive effect on the cooling power produced but a negative effect on the electricity production (Figure 9).

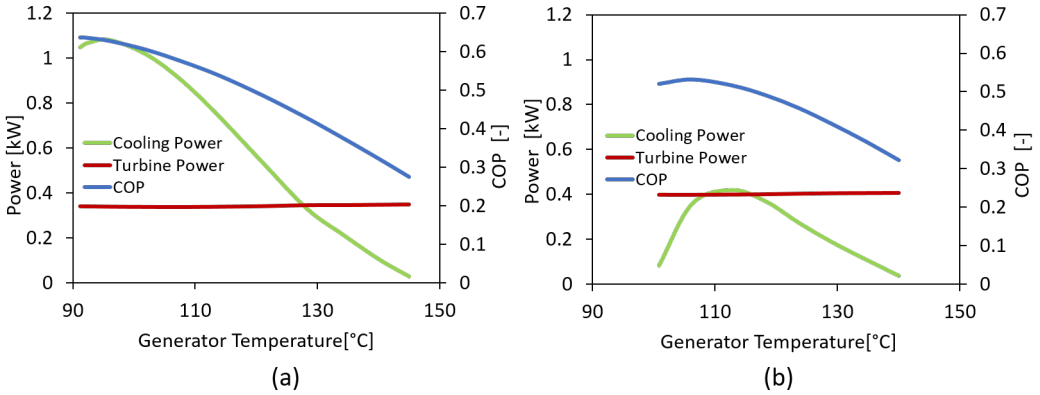

Figure 7. Generator Temperature influence for a cooling production at 5°C (a) and -5°C (b)

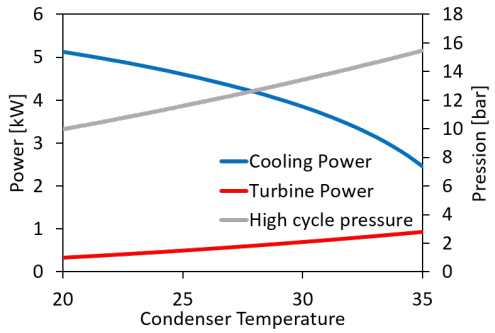

Figure 8. Condenser temperature influence for a power supply at the generator of 15 kW at 100°C and evaporator temperature of 5°C

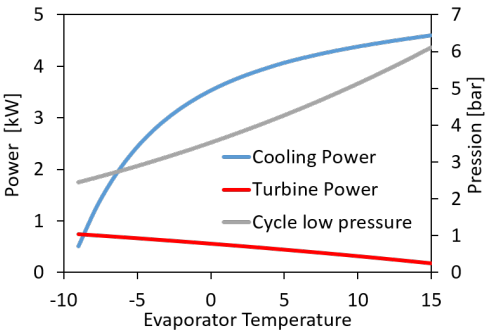

Figure 9. Evaporator temperature influence for a power supply at the generator of 15 kW at 100°C and ambient temperature of 25°C

Finally, for direct comparison of the cooling and electric power produced in different operating conditions, efficiency was expressed in simplified exergetic terms. The exergy efficiency of the cycle was expressed as follows

$$\eta_{II,cycle} = \eta_{II,cold} \cdot r_s + \eta_{II,power} \cdot (1 - r_s) \tag{8}$$

Where:

$$\eta_{II,cold} = \frac{COP}{COP_{Carnot}} \tag{9}$$

$$COP_{Carnot} = \frac{T_e \cdot (T_g - T_c)}{T_g \cdot (T_c - T_e)} \tag{10}$$

$$\eta_{II,power} = \frac{\eta_I}{\eta_{Carnot}} \tag{11}$$

$$\eta_{Carnot} = 1 - \frac{T_c}{T_g} \tag{12}$$

As an example, the below given figure shows how, for a generator temperature of 100°C, decreasing the evaporator temperature increases the power produced by the turbine while it decreases the cooling power produced, but a maximum of the second principle efficiency for the system can be found at around -5°C. In the same way, fixing a desired temperature for the cold production, an optimum generator temperature, maximizing the second principle efficiency, can be found.

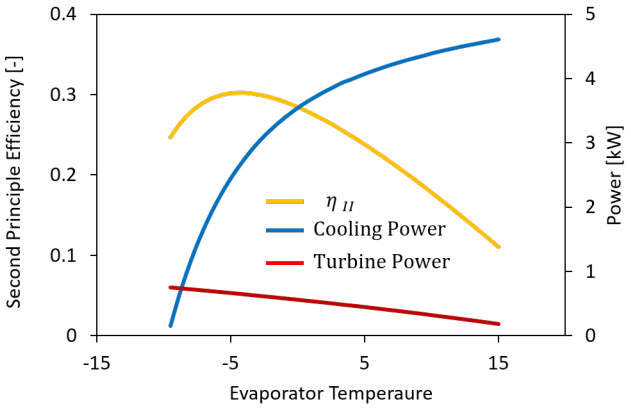

Figure 10. Cycle performance as a function of the evaporator temperature for a power input of 15 kW at 100°C at the generator and an ambient temperature of 25 °C

5 Conclusions

An impulse turbine has a number of advantages compared to volumetric expanders, including the lower influence of leaking losses, which play a large role in very small machines.

The expander achieves chocking conditions with low expansion ratios, above which the mass flow rate in the turbine no longer changes. The power produced by the turbine is highly dependent on its rotation speed and optimum operation appears to be around 50,000 - 70,000 rpm depending on operating conditions.

The increase in temperature of the hot source feeding the generator seems to have no major effect on the power produced by the turbine because it is accompanied by a reduction in the treated mass flow rate. On the other hand, the influence of the temperature of the condenser (generally cooled by the ambient air) seems strong on the electricity and cooling production which are respectively proportional and inversely proportional to the intermediate source temperature. The evaporator temperature turns out to be the most influential parameter: its reduction has a positive effect on electricity production and a negative one on cooling production, thus emphasizing the importance of a preliminary definition of the cooling production temperature when designing the system. This defined, the generator temperature can be set in order to maximise the power production, the cooling production or second principle efficiency.

Finally, in the lack of possibility of regulating its mass flow, the turbine sets strict limits in terms of acceptable operating conditions for the cycle. For this reason, the addition of a regulation system to the model is being studied for application to the experimental setup.

Aknoledgments: The authors would like to express their gratitude to the French Alternative Energies and Atomic Energy Commission and the Carnot Energies of the Future Institute. S. Braccio was supported by the CEA NUMERICS program, which has received funding from the European Union's Horizon 2020 research and innovation program under the Marie Sklodowska-Curie grant agreement No 800945.

References

[1] K.E. Herold, R. Radermacher, S.A. Klein, *Absorption Chillers and Heat Pumps* (2016)
[2] D.S. Ayou, J.C. Bruno, R. Saravanan, A. Coronas, *An overview of combined absorption power and cooling cycles* (2013)
[3] A. Khaliq, Applied Thermal Engineering **112**, 1305 (2017)
[4] F. Xu, D. Yogi Goswami, S. S. Bhagwat, Energy (2000)
[5] G.P. Kumar, R. Saravanan, A. Coronas, Energy **128**, 801 (2017)
[6] J. Wang, Y. Dai, T. Zhang, S. Ma, Energy **34**, 1587 (2009)
[7] N. Voeltzel, H.T. Phan, N. Tauveron, B. Gonzalez, Q. Blondel, M. Wirtz, F. Boudehenn, Proceedings of the ISES Solar World Congress 2019 and IEA SHC International Conference on Solar Heating and Cooling for Buildings and Industry 2019 pp. 2681–2690 (2020)
[8] J. Muye, D.S. Ayou, R. Saravanan, A. Coronas, Applied Thermal Engineering **97**, 59 (2016)
[9] L.C. Mendoza, D.S. Ayou, J. Navarro-Esbrí, J.C. Bruno, A. Coronas, Applied Thermal Engineering **72**, 258 (2014)
[10] G.K. Alexis, International Journal of Refrigeration **30**, 1097 (2007)
[11] A. Landelle, N. Tauveron, P. Haberschill, R. Revellin, S. Colasson, Applied Energy (2017)
[12] F. Boudéhenn, H. Demasles, J. Wyttenbach, X. Jobard, D. Chèze, P. Papillon, Energy Procedia **30**, 35 (2012)
[13] N. Voeltzel, H.T. Phan, Q. Blondel, B. Gonzalez, N. Tauveron, Thermal Science and Engineering Progress **19**, 100650 (2020)
[14] Q. Blondel, N. Tauveron, N. Caney, N. Voeltzel, Applied Sciences (Switzerland) (2019)
[15] E. Balje (1962)
[16] *EES: Engineering Equation Solver|F-Chart Software:Engineering Software*, http://www.fchart.com/ees/, accessed on 27 June 2021
[17] S. Ibrahim, O.M., Klein, *Thermodynamic properties of ammonia-water mixtures.*, in *ASHRAE Trans.: Symposia, 21, 2, 1495* (1993)
[18] J.D. Anderson (1982)
[19] S. Dixon, C. Hall, *Fluid Mechanics and Thermodynamics of Turbomachinery* (2010), ISBN 9781856177931
[20] S.Y. Cho, C.H. Cho, C. Kim, JSME International Journal, Series B: Fluids and Thermal Engineering **49**, 1290 (2007)
[21] J.P. Czapla (2015)
[22] M.H. Vavra, *Aero-Thermodynamics and Flow in Turbomachines* (John Wiley, 1960)
[23] A. Capetti, *Motori termici* (UTET, 1964)